







## Shear-induced anomalous transport and charge asymmetry of triangular flow in heavy-ion collisions

Matteo Buzzegoli <sup>1,\*</sup> Dmitri E. Kharzeev <sup>2,3,†</sup> Yu-Chen Liu <sup>2,4,‡</sup> Shuzhe Shi <sup>2,§</sup>  
Sergei A. Voloshin <sup>5,¶</sup> and Ho-Ung Yee <sup>6,\*\*</sup>

<sup>1</sup>*Department of Physics and Astronomy, Iowa State University, Ames, Iowa 50011, USA*

<sup>2</sup>*Center for Nuclear Theory, Department of Physics and Astronomy, Stony Brook University, Stony Brook, New York 11794-3800, USA*

<sup>3</sup>*Department of Physics, Brookhaven National Laboratory, Upton, New York 11973-5000, USA*

<sup>4</sup>*Physics Department and Center for Field Theory and Particle Physics, Fudan University, Shanghai 200433, China*

<sup>5</sup>*Department of Physics and Astronomy, Wayne State University, 666 W. Hancock, Detroit, Michigan 48201, USA*

<sup>6</sup>*Physics Department, University of Illinois at Chicago, Chicago, Illinois 60607, USA*



(Received 2 August 2022; accepted 17 October 2022; published 18 November 2022)

Chiral anomaly implies the existence of nondissipative transport phenomena, such as the chiral magnetic effect. At second order in the derivative expansion, novel quantum transport phenomena emerge. In this paper, we focus on the anomalous transport driven by a combination of shear, vorticity, and magnetic field. We find that the corresponding transport phenomena—shear-induced chiral magnetic and chiral vortical effects—induce characteristic charge correlations among the hadrons produced in heavy ion collisions. We propose the charge asymmetry of triangular flow as a signature of the anomalous transport, and estimate the strength of the signal, as well as the background, using hydrodynamical model simulations. We find that the signal-to-background ratio for the proposed observable is favorable for experimental detection.

DOI: [10.1103/PhysRevC.106.L051902](https://doi.org/10.1103/PhysRevC.106.L051902)

*Introduction.* The chiral anomaly links the short distance behavior of chiral fermions in quantum field theory to the macroscopic properties of the gauge fields that can possess nontrivial topology. As a result, new kinds of transport phenomena emerge in systems possessing chiral fermions in the presence of magnetic field or vorticity, see [1–6] for reviews. The most studied phenomena of this type are the chiral magnetic effect (CME) [7–9] and the chiral vortical effect (CVE) [10,11] that describe nondissipative transport of electric charge along the axis of magnetic field or vorticity in the presence of chirality imbalance. In addition, at finite vector charge density (e.g., at a finite baryon number density), quantum anomalies induce the axial current in response to both magnetic field and vorticity [12–14]. The vector and axial currents are coupled by the chiral anomaly, which leads to the

emergence of a novel collective excitation, the chiral magnetic wave [15].

The generation of axial current may be related [16–18] to the recently observed polarization of  $\Lambda$  hyperons in heavy ion collisions at the BNL Relativistic Heavy Ion Collider (RHIC) [19]. In particular, the measurement of the second order harmonic in the azimuthal angle dependence of longitudinal (along the beam axis)  $\Lambda$  polarization [20,21] points towards a substantial role of the shear-induced mechanism of polarization [22,23]. This raises a question of whether the chiral anomaly may induce a higher harmonic in the azimuthal distribution of electric charge.

Indeed, such effects were predicted to arise at the second order in the gradient expansion in hydrodynamics as a consequence of chiral anomaly [24]. Specifically, the electric current was predicted to possess contributions from shear in the presence of vorticity and magnetic field, and a contribution from the combination of vorticity and magnetic field. The corresponding transport coefficients are proportional to the chiral chemical potential, just like for the CME and CVE, so these effects can be considered as the second-order analogs of CME and CVE. These effects were studied using the effective field theory methods in [25].

*Second order anomalous transport coefficients.* The CME and CVE are of first order in the hydrodynamic gradient expansion, and the corresponding transport coefficients can be derived in the framework of hydrodynamics by imposing the non-negativity of entropy production [26]. At second order, there appear additional transport coefficients that have been classified in Ref. [24]. The relations between these transport

\*mbuzz@iastate.edu

†dmitri.kharzeev@stonybrook.edu

‡yu-chen.liu@stonybrook.edu

§shuzhe.shi@stonybrook.edu

¶sergei.voloshin@wayne.edu

\*\*hyee@uic.edu

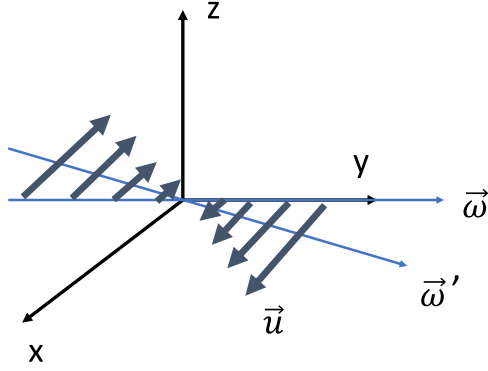


FIG. 1. The tilting of vorticity in a shear flow. In the presence of a shear flow  $\sigma^{xy}$  (the fluid velocity  $\mathbf{u}$  is along  $\mathbf{x}$  with  $\partial u^x/\partial y \neq 0$ ), the vortex immersed in the flow and originally pointing in the direction  $\boldsymbol{\omega} \sim \mathbf{y}$  gets tilted and points in the direction  $\boldsymbol{\omega}'$ , thus acquiring a component along  $\mathbf{x}$ .

coefficients have been derived from the *absence* of entropy production that stems from the time reversal invariance [24].

In this paper we will focus on the contributions to electric current that arise from the combination of shear and vorticity or magnetic field [24]:

$$j_{(2)}^\mu = \xi_1 \sigma^{\mu\nu} \omega_\nu + \xi_2 Q \sigma^{\mu\nu} B_\nu, \quad (1)$$

where  $\sigma^{\mu\nu} = \frac{1}{2}(\partial_\perp^\mu u^\nu - \partial_\perp^\nu u^\mu)$  is the transverse shear tensor ( $u^\mu$  is the fluid velocity and  $\partial_\perp^\mu$  is the gradient perpendicular to  $u^\mu$ ),  $\omega^\mu = \frac{1}{2}\epsilon^{\mu\nu\alpha\beta} u_\nu \partial_\alpha u_\beta$  is vorticity, and  $B^\mu$  is magnetic field. We will refer to the first term in Eq. (1) as the shear-induced chiral vortical effect (siCVE), and to the second term as the shear-induced chiral magnetic effect (siCME).<sup>1</sup>

What is the microscopic origin of the phenomena encoded in Eq. (1)? It is well known that the anomaly relation, and thus the expression for the CME current

$$\mathbf{j} = \frac{e^2}{2\pi^2} \mu_5 \mathbf{B}, \quad (2)$$

are exact *at the operator level*. Nevertheless, when the expectation value of this operator relation is taken over a physical state, there may well appear corrections arising from the renormalization of operator quantities that enter Eq. (2), see, e.g., [27] and discussion in [28]. In particular, the magnetic field in the medium can be renormalized by interactions. Moreover, if the shear (and/or vorticity) are present in the medium, they can rotate the orientation of an effective magnetic field by generating a component of the field in the direction perpendicular to initial  $\mathbf{B}$ .

To illustrate this argument, let us consider a vortex immersed in the flow and aligned initially along the axis  $y$ , with  $\boldsymbol{\omega} \sim \hat{\mathbf{y}}$ . The shear flow with  $\sigma^{xy} \sim \omega_z$  will rotate the axis of the vortex in the  $(x, y)$  plane, creating a component of an effective vorticity along the axis  $x$ , see Fig. 1. This “tilting” of vorticity in shear flows has been extensively studied in hydrodynamics,

see [29] and references therein. Perhaps the most spectacular manifestation of vorticity tilting in nature is the emergence of tornadoes in “supercell” thunderstorms, see [30] for a review.

The “conventional” first order chiral vortical effect will then create the current along the  $x$  axis. Therefore, the second order anomalous transport phenomenon can be understood in terms of the modification of vorticity (or magnetic field) by the back-reaction of the medium.

The values of the second-order transport coefficients  $\xi_i$  had been evaluated at strong and weak coupling through holography and chiral kinetic theory, respectively. These computations will be briefly summarized below. One can also write down the general Kubo relations for these coefficients that will be described below as well.

*Transport coefficients at strong coupling.* The value of  $\xi_1$  has been computed by holographic methods in  $N = 4$  supersymmetric Yang-Mills (SYM) theory [11]. Although the conformal  $N = 4$  SYM and quantum chromodynamics (QCD) are clearly not the same theories, we may estimate  $\xi_1$  for QCD basing on the  $N = 4$  SYM result. We thus get

$$\xi_1 = -\frac{N_F N_c}{\sqrt{3}\pi^3} \frac{\mu_A \mu}{T} \quad (\text{strong coupling}), \quad (3)$$

where  $\mu$  and  $\mu_A$  are the chemical potentials of the vector and axial charges, respectively. For numerical estimates we will assume that the number of light quark flavors  $N_F = 3$ .

Considering parity and charge conjugation symmetries,  $\xi_2$  is proportional to  $\mu_A$  only, and we estimate

$$\xi_2 = -\frac{N_F N_c}{\sqrt{3}\pi^3} \frac{\mu_A}{T} \quad (\text{strong coupling}). \quad (4)$$

It is interesting to note that these transport coefficients are the result of interplay between chiral anomaly and the dissipative dynamics of the plasma represented by shear viscosity and conductivity. This physics seems to be unique for these transport terms, among other possible second order terms. This feature will be important in our computation of these transport coefficients in weakly coupled regime, and also in the derivation of Kubo relations based on the Zubarev approach.

*Weakly coupled regime: The chiral kinetic theory.* To demonstrate the universal nature of the discussed phenomenon, let us now discuss how it emerges at weak coupling. For this purpose we will present a derivation of shear-induced anomalous transport using the chiral kinetic theory (CKT) [31–33].

Using the covariant fermion Wigner function

$$W_{ab}(x, p) = \int d^4 y e^{\frac{i}{\hbar} p \cdot y} \langle \bar{\psi}_b(x) e^{y \cdot \nabla} e^{-y \cdot \nabla} \psi_a(x) \rangle, \quad (5)$$

where  $\nabla_\mu \psi = (\partial_\mu + i Q A_\mu / \hbar) \psi$ , we can express the vector current in the form  $j^\mu = \int \frac{d^4 p}{(2\pi)^4} \text{Tr}[\gamma^\mu W(x, p)]$ .

Dirac equation for charged massless fermions in a constant electromagnetic field leads to the following equation for the Wigner function:

$$\gamma^\mu \left( p_\mu + \frac{i\hbar}{2} \Delta_\mu \right) W(x, p) = 0, \quad (6)$$

<sup>1</sup>This effect, introduced in [24], is referred to as shear-induced Hall effect in Ref. [25].

where  $\Delta_\mu = \partial_\mu - Q F_{\mu\lambda} \partial_\rho^\lambda$ ; we regard the electromagnetic field  $F^{\mu\nu}$  as the first order quantity in the derivative expansion.

We are interested in the vector current that represents the sum of right-handed and left-handed chiral currents:  $j^\mu = j_+^\mu + j_-^\mu$ . The right- and left-handed currents of charge  $Q$  fermions with (dual) electromagnetic field  $\tilde{F}^{\mu\nu}$  are given in CKT by

$$j_\mu^\pm = \int \frac{d^4 p}{(2\pi)^4} [4\pi \delta(p^2) p_\mu f^\pm + \tilde{\mathcal{J}}_\mu^\pm + \tilde{\mathcal{J}}_\mu^{\pm\sigma}] \quad (7)$$

with

$$\begin{aligned} \tilde{\mathcal{J}}_\mu^\pm &\equiv 4\pi \hbar \delta(p^2) \left\{ \mp \frac{Q}{p^2} \tilde{F}_{\mu\sigma} p^\sigma f^\pm \pm \Sigma_{\mu\rho}^n \Delta^\rho f^\pm \right\}, \\ \tilde{\mathcal{J}}_\mu^{\pm\sigma} &\equiv \mp p_\mu \frac{1}{p^2} \frac{\hbar}{2pn} \epsilon_{\alpha\beta\rho\sigma} p^\alpha n^\beta \Delta^\rho \tilde{\mathcal{J}}_\pm^\sigma \\ &\quad \pm \frac{\hbar}{2pn} \epsilon_{\mu\nu\rho\sigma} n^\nu \Delta^\rho \tilde{\mathcal{J}}_\pm^\sigma, \end{aligned} \quad (8)$$

where  $f^\pm$  is the distribution function for right(left)-handed particles,  $\Sigma_n^{\mu\nu} \equiv \epsilon^{\mu\nu\rho\sigma} p_\rho n_\sigma / (2pn)$  is a spin tensor for chiral fermions, and  $n^\mu$  is a unit time-like frame that satisfies  $n^2 = 1$ . The second-order expressions for the current have also been derived, both for the case of background electromagnetic field [34] and for a curved space-time in Ref. [35].

According to the analysis [24], the shear-induced second order terms are given by Eq. (1). We find that such terms do not arise from  $\tilde{\mathcal{J}}_\mu^\pm$ . This is consistent with the qualitative analysis given above that indicates that these shear-induced terms originate from the medium modifications of the distribution function. We will see below that once these modifications are taken into account in the first order distribution function  $f_{(1)}^\pm$ , the shear-induced current indeed emerges from  $\tilde{\mathcal{J}}_\mu^\pm$ .

We assume, as usual, that the distribution function depends on the linear combination of quantities that are collisionally conserved at local equilibrium, so that the detailed balance condition can be satisfied. For the case of Fermi-Dirac distribution we thus obtain [36]

$$f_{\text{eq}}^\pm = [e^{(p \cdot \beta \mp \frac{\hbar}{2} \Sigma_n^{\alpha\beta} \gamma_{\alpha\beta} - \alpha^\pm)} + 1]^{-1}, \quad (9)$$

where  $\alpha^\pm = \mu^\pm / T$  and  $\beta_\mu = u_\mu / T$  are, respectively, the temperature-scaled chemical potential and fluid velocity, and  $\gamma_{\alpha\beta} = -\frac{1}{2}(\partial_\alpha \beta_\beta - \partial_\beta \beta_\alpha)$  is thermal vorticity. The above distribution function agrees with the one obtained within the exact density matrix approach [37] at first order in vorticity; we can thus use it to describe the effects at first order in vorticity. An important point for us is that there is no shear-induced term in  $f_{\text{eq}}^\pm$ , which means that we cannot derive second order shear-induced terms in  $\tilde{\mathcal{J}}_\mu^\pm$  using the distribution function (9).

In order to include the shear contributions, we need to consider the viscous corrections to the distribution function. For this purpose, we employ the moment expansion method [38] to formulate the nonequilibrium distribution:

$$f^\pm = f_{\text{eq}}^\pm + f_{\text{eq}}^\pm (1 - f_{\text{eq}}^\pm) (\lambda_\Pi^\pm \Pi + \lambda_\nu^\pm v_\pm^\mu p_\mu + \lambda_\pi^\pm \pi^{\mu\nu} p_\mu p_\nu), \quad (10)$$

and compute the shear-induced chiral transport coefficients. Here,  $\lambda_X^\pm$  are polynomials of  $up$ , with coefficients being func-

tions of  $T$  and  $\alpha^\pm$ . They are determined by matching the energy-momentum stress tensor from its microscopic integral representation to the corresponding macroscopic viscous terms. Following this approach, we find that (the details of the derivation are presented in the Supplemental Material [39])

$$\begin{aligned} \xi_1 &\approx -0.62 \frac{\eta}{s} \frac{\mu_A \mu}{T} = -0.05 \frac{\mu_A \mu}{T} \quad (\text{weak coupling}), \\ \xi_2 &\approx -6.70 \frac{\eta}{s} \frac{\mu_A}{T} = -0.53 \frac{\mu_A}{T} \quad (\text{weak coupling}), \end{aligned} \quad (11)$$

where  $\eta$  is a shear viscosity, and  $s$  is an entropy density.

While the relations (11) have been obtained within the chiral kinetic theory that is applicable at weak coupling, the second equalities in Eq. (11) are based on the assumption  $\eta/s = 1/(4\pi)$  that follows from holography at strong coupling and is favored by the data. The use of weak coupling value of  $\eta/s$  would yield substantially bigger values of the transport coefficients  $\xi_1$  and  $\xi_2$ —so the values (11) can be considered as lower bounds on these quantities at weak coupling. Let us note that the  $\xi$  coefficients have been computed in Ref. [40] using relaxation time approximation, as well as using moment expansion method in Ref. [41] for a single-component fluid.

*Kubo relations in the Zubarev approach.* It is important to establish the general Kubo formulas for the transport coefficients of siCME and siCVE. For a relativistic quantum system, Kubo relations can be obtained using the linear response theory in the Zubarev formalism for the nonequilibrium statistical operator [42,43].

In this formalism, a covariant form of the local thermal equilibrium statistical operator is obtained by maximizing the total entropy at fixed energy-momentum density [44–48]. In the presence of vorticity the statistical operator around a point  $x$  can be approximated as [49]

$$\hat{\rho} \simeq \frac{1}{Z} \exp\{-\beta(x)\hat{P} + \hat{B}_\omega + \hat{B}_D\}$$

with  $\hat{P}$  the total momentum of the system and

$$\hat{B}_\omega = -\beta(x) \omega_\rho(x) \hat{J}_x^\rho, \quad \hat{B}_D = \int_\Omega d\Omega \hat{T}^{\mu\nu} \nabla_\mu \beta_\nu,$$

where  $\hat{J}_x$  is the angular momentum of the system evaluated around the point  $x$  and  $\Omega$  is the region of space-time enclosed by the two hypersurfaces at the initial thermalization time and at the present time, and by the time-like hypersurface at their boundaries. The operator  $\hat{B}_\omega$  describes the nondissipative effects related to vorticity, while  $\hat{B}_D$  describes the dissipative effects. In particular, the latter contains the contribution from the shear tensor that can be written as  $\hat{B}_\eta = \int_\Omega d\Omega \hat{T}^{\mu\nu} \beta_{\sigma\mu\nu}$ .

The siCVE is obtained by evaluating the current  $j^\mu(x) = \text{tr}[\hat{\rho} \hat{j}^\mu(x)]$  as a linear response to  $\hat{B}_\omega$  and  $\hat{B}_D$  and considering the term of order  $\hat{B}_\omega \times \hat{B}_\eta$ . Using the linear response theory as in [50–56] and expressing the correlators in terms of the three-point retarded Green function [57–59]

$$\begin{aligned} &iG_{\hat{O}, \hat{X}, \hat{Y}}^{\text{R1}}(x; x_1, x_2) \\ &= \theta(t - t_1) \theta(t_1 - t_2) \langle [ [\hat{O}(x), \hat{X}(x_1)], \hat{Y}(x_2)] \rangle_T \\ &\quad + \theta(t - t_2) \theta(t_2 - t_1) \langle [ [\hat{O}(x), \hat{Y}(x_2)], \hat{X}(x_1)] \rangle_T, \end{aligned}$$

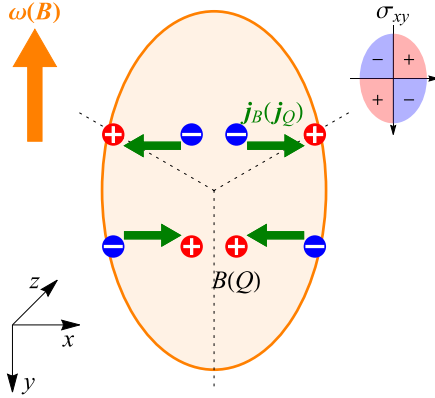


FIG. 2. Illustration of the shear-induced chiral vortical and magnetic effects; see text for the description.

we obtain (see Supplemental Material [39] for detailed derivation)

$$\Delta_{\omega\eta} j^\mu(x) = \frac{2\omega_v(x)}{\beta(x)} \int d^4x_1 \int d^4x_2 \int_{-\infty}^{\tau_2} d\theta_2 \beta(x_2) \sigma^{\mu\nu}(x_2) \times (x_1 - x)^y i G_{\hat{j}^y, \hat{T}^{tz}, \hat{T}^{xy}}^{\text{R1}}(x; x_1, (\theta_2, \mathbf{x}_2)),$$

where we denoted by  $(\widehat{O})_T$  the trace with the homogeneous statistical operator in the local rest frame with temperature  $T = 1/\beta(x)$ . Notice that since the effects that we seek to describe require breaking of parity, this statistical operator must also contain a chiral imbalance.

We can move the shear tensor out of the integration by studying the perturbations with respect to the equilibrium. For a fluid in the hydrodynamic regime, only the perturbations with small frequency and small wave vector contribute to the integral. In that case, following [43], we obtain  $\Delta_{\omega\eta} j^\mu(x) = \sigma^{\mu\nu}(x) \omega_\nu(x) \xi_1$  with

$$\xi_1 = \lim_{p, q \rightarrow 0} 2 \frac{\partial}{\partial q^0} \frac{\partial}{\partial p^y} \text{Im} G_{\hat{j}^y, \hat{T}^{tz}, \hat{T}^{xy}}^{\text{R1}}(p, q), \quad (12)$$

where  $G^{\text{R1}}(p, q) = \int d^4x_1 d^4x_2 e^{-i(p \cdot x_1 + q \cdot x_2)} G^{\text{R1}}(0; x_1, x_2)$ . Moreover, comparing the known Kubo formulas of the CME and CVE, we see that we can obtain  $\xi_2$  from  $\xi_1$  replacing  $\hat{T}^{tz}$  with  $(\beta/2)\hat{j}^z$ , that is

$$\xi_2 = \lim_{p, q \rightarrow 0} \beta \frac{\partial}{\partial q^0} \frac{\partial}{\partial p^y} \text{Im} G_{\hat{j}^y, \hat{j}^z, \hat{T}^{xy}}^{\text{R1}}(p, q). \quad (13)$$

*Experimental observable: Charge dependent fluctuations of  $a_3$ .* Let us now discuss the experimental signatures of siCME and siCVE. Let us assume that the beam direction of the colliding ions is along the axis  $\mathbf{z}$ , and the axis  $\mathbf{x}$  lies in the reaction plane, see Fig. 2. The elliptical flow of the expanding quark-gluon plasma then induces the dependence of the fluid velocity component  $u_x$  on  $y$ , and thus the shear  $\sigma_{xy}$  of the sign that is indicated in the insert of Fig. 2. The axes of vorticity and magnetic field are aligned perpendicular to the reaction plane, anti-parallel to  $\mathbf{y}$ . The resulting siCME and siCVE currents are thus directed parallel or antiparallel to  $\mathbf{x}$ , depending on the sign of  $\sigma_{xy}$ , as shown in Fig. 2.

As a result, the siCME, i.e., the current term  $\xi_2 \sigma^{\mu\nu} B_\nu$ , would lead to the triangular distortion of the particle momentum distribution, that will be different for positive and negative particles. The sign of this distortion for positive and negative particles will fluctuate event-by-event, reflecting the fluctuations of the chiral chemical potential  $\mu_A$ . This is similar to the charge-dependent dipole distortion of the momentum distribution induced by the ‘‘conventional’’ CME.

The azimuthal particle distribution in heavy ion collision is often parametrized with Fourier series:

$$\frac{dN}{d\phi} \propto 1 + \sum_{n=1}^{\infty} [2v_n \cos(\Delta\phi) + 2a_n \sin(\Delta\phi)], \quad (14)$$

where  $\Delta\phi = \phi - \Psi_{\text{RP}}$  is the emission angle relative to the reaction plane. Coefficients  $a_n$  are zero if parity is conserved in the collision. Experimental search for the conventional CME is focused on measuring correlators sensitive to the product  $\langle a_{1,\alpha} a_{1,\beta} \rangle$  where  $\alpha$  and  $\beta$  denote the charge of the particles [60]. It is usually done by measuring the so-called ‘‘gamma’’ correlator  $\gamma_1^{\alpha\beta} = \langle \cos(\phi_\alpha + \phi_\beta - 2\Psi_{\text{RP}}) \rangle$ .

The charge-dependent triangular distortions of the momentum distributions can be detected by the third order sine harmonics  $a_3 \equiv \langle \sin(3\phi - 3\Psi_{\text{RP}}) \rangle$  evaluated for particles with positive  $a_3^+$  and negative  $a_3^-$  charges. Namely,  $a_3^+ = -a_3^- \neq 0$  in each event, where the sign of  $a_3^+$  depends on the sign of chiral imbalance.

In analogy to the ‘‘conventional’’ CME observables, we thus define the two-particle correlator of third order harmonics,  $\gamma_3^{\alpha\beta} \equiv \langle \cos(3\phi_\alpha + 3\phi_\beta - 6\Psi_{\text{RP}}) \rangle$ . This correlator for same-sign (SS) and opposite-sign (OS) pairs responds to the effect as follows:  $\gamma_3^{\text{SS}} = \gamma_{3,\text{bkg}}^{\text{SS}} - (a_3^+)^2$  and  $\gamma_3^{\text{OS}} = \gamma_{3,\text{bkg}}^{\text{OS}} + (a_3^+)^2$ , where  $\gamma_{3,\text{bkg}}$  represents the background contributions. Therefore, the difference  $\Delta\gamma_3 \equiv \gamma_3^{\text{OS}} - \gamma_3^{\text{SS}}$  should be sensitive to the siCME.

For the siCVE, induced by the current term  $\xi_1 \sigma^{\mu\nu} \omega_\nu$ , the analysis is very similar, but one expects it to lead mostly to the separation of baryons and antibaryons, just as for the CVE [61].

To estimate the signal, we use the AVFD simulation framework [62–64] to evaluate the vector and axial-vector charge evolution on top of a realistic hydrobackground with axial charge initial condition  $|n_A/s| = 0.1$  (equivalently,  $|\mu_A/T| \sim 1$ ) and magnetic field lifetime  $\tau_B = 1$  fm. The magnitude and the spatial distribution of the initial chirality imbalance are set to be the same as in the CME simulation. Even if the size of topological fluctuations is small, the assumption of a uniform distribution may still capture the average effect resulting from the random diffusion of topological charge that leads to Chern-Simons number of order  $\sqrt{N}$ , where  $N$  is the number of sphalerons. The initial profile of the magnetic field is computed from the initial proton distribution of the colliding nuclei. The bulk evolution starts from the event-averaged Monte Carlo Glauber initial conditions, followed by solving 2+1 dimensional second-order viscous hydrodynamic equations with MUSIC [65,66].

We focus on top energy  $\sqrt{s_{NN}} = 200$  GeV Au+Au collisions and compute the observables proposed above for the detection of shear-induced chiral effects. As an example, we

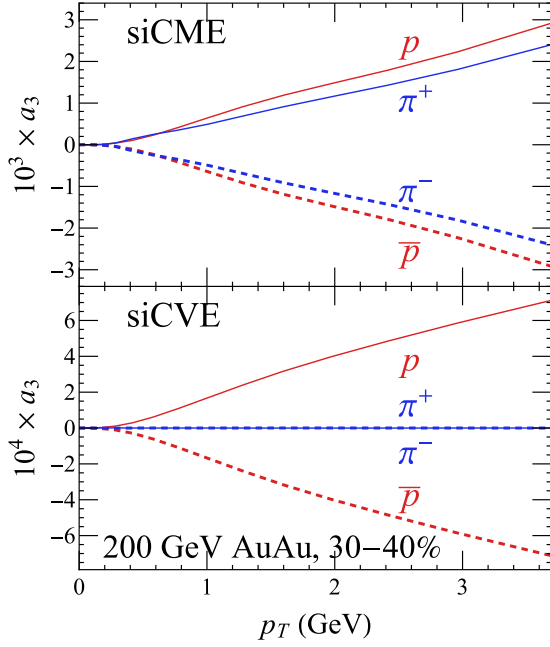


FIG. 3. (Upper) Transverse momentum dependence of third-harmonic charge separation for  $\pi^+$ ,  $\pi^-$ ,  $p$ , and  $\bar{p}$  due to the shear-induced chiral magnetic effect. (Lower) Same as the upper panel but for the shear-induced chiral vortical effect.

take an event with an excess of right-handed particles ( $n_5 > 0$ ), and show the transverse momentum dependence of the  $a_3$  moments. The cases of siCME and siCVE are shown in the upper and lower panels of Fig. 3, respectively. We observe a  $\mathcal{O}(10^{-3})$  difference between  $a_3^{\pi^+}$  and  $a_3^{\pi^-}$  ( $a_3^p$  and  $a_3^{\bar{p}}$ ) due to the siCME(siCVE) effect, and the separation increases with transverse momentum  $p_T$ . We find that the contribution from “conventional” CME to  $a_3$  is an order of magnitude smaller than the contribution from siCME.

The amplitude of the signal in  $a_3$  is smaller than the CME  $a_1$  charge separation by an order of magnitude, as appropriate for a second-order effect in the hydrodynamical derivative expansion. It is thus especially important to estimate the nonchiral effect of the background on  $\Delta\gamma_3$  before a conclusion on observability of siCME and siCVE in heavy-ion collisions can be reached.

To estimate the background from resonance decays, we sample the resonances according to their transverse distribution,  $\frac{dN^{\text{res}}}{d p_T d\phi}$ , and collect the decay particle pairs that fall into the kinematic region of interest that is chosen to be  $0.5 < p_T < 2$  GeV and  $|\eta| < 0.5$ . The lower  $p_T$  cut is chosen to enhance the signal and suppress the background. We include the two-particle decay of  $K_S^0$ ,  $\rho^0$ , and  $\omega$  and three-particle decay of  $K_L^0$ ,  $\eta$ , and  $\omega$  particles.

Noting that for resonance decays  $\langle \cos(3\phi_\alpha + 3\phi_\beta - 6\Psi_{\text{RP}}) \rangle \approx \langle \cos(3\phi_\alpha + 3\phi_\beta - 6\phi^{\text{res}}) \cos(6\phi^{\text{res}} - 6\Psi_{\text{RP}}) \rangle \approx \langle \cos(3\phi_\alpha + 3\phi_\beta - 6\phi^{\text{res}}) \rangle v_{6,\text{RP}}^{\text{res}}$  and similarly for local-charge conservation [67,68], we expect that the background contribution in  $\Delta\gamma_3$  is proportional to the sixth-order flow harmonic with respect to the reaction plane (or the second-order event plane). In Fig. 4, we present the centrality dependence of

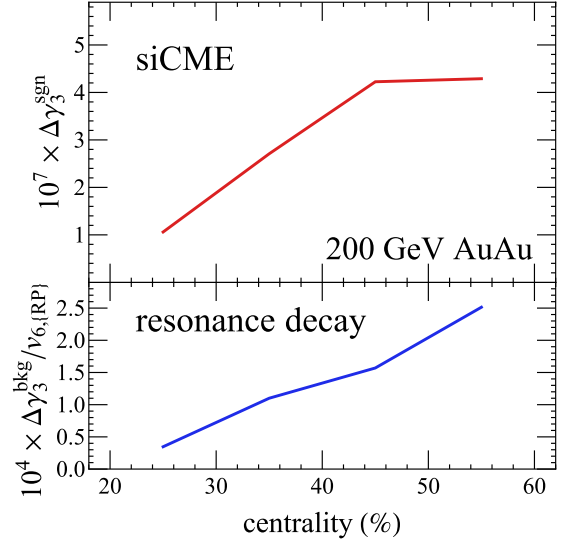


FIG. 4. Centrality dependence of two-point correlation  $\Delta\gamma_3$  induced by shear-induced chiral magnetic effect (upper) and resonance decay background (lower).

siCME signal ( $\Delta\gamma_3^{\text{sgn}} \equiv 2a_3^2$ ) and the background induced by resonance decay, with the latter scaled by  $v_{6,\text{RP}}$ . In the event-by-event hydrosimulation, we found that  $v_{6,\text{RP}}$  is within  $\mathcal{O}(10^{-4})$ , which makes  $\Delta\gamma_3^{\text{bkg}} \sim \mathcal{O}(10^{-8})$ . As has been found in the simulation of CME, resonance decays contribute to about  $\sim 50\%$  of the non-CME background. Therefore, although some other possible backgrounds, e.g. the local charge conservation, are not included in the current estimation, we expect the overall background to be of the same order as what is shown here. Hence, we predict that the signal  $\Delta\gamma_3^{\text{sgn}} \sim \mathcal{O}(10^{-7})$  may be significantly (by an order of magnitude) greater than the background.

*Discussion.* While the magnitude of the observable  $\Delta\gamma_3^{\text{sgn}} \sim \mathcal{O}(10^{-7})$  induced by siCME and siCVE is about two orders of magnitude smaller than for “conventional” CME and CVE, it is expected to be much less contaminated by the background. This is because the resonance decays and local charge conservation contribute a lot less to this observable than to the “conventional”  $\gamma$  correlator.

The expected dominance of the signal over the background (about an order of magnitude) should make siCME and siCVE detectable in heavy ion collisions with high statistics data samples. We thus urge the experimental studies of siCME and siCVE in both AuAu and isobar collisions at RHIC (even though we do not predict an observable *difference* between the two isobar pairs, the effects could be detectable in both isobars with the presently accumulated statistics). It will also be of interest to investigate the effect at the CERN Large Hadron Collider.

It would be interesting to search for siCME and siCVE at lower collision energies during the beam energy scan. One may expect the enhancement of these effects due to the larger baryon chemical potential, possibly larger vorticity [69], longer-lived magnetic field, and the enhancement of

topological fluctuations [70] due to proximity to the critical point of the QCD phase diagram [71,72].

In the future, it will be interesting to investigate the contribution, analogous to siCME and siCVE, of anomalous shear-induced axial currents to the polarization of  $\Lambda$  hyperons. In particular, the proportionality of the corresponding transport coefficients to the square of the chemical potential  $\mu^2$  can yield a characteristic dependence of polarization on the charge asymmetry of the event. It would also be important to check

our predictions for the siCME and siCVE transport coefficients using lattice QCD and the Kubo relations derived here.

*Acknowledgments.* This work is supported by the U.S. Department of Energy, Office of Science, Office of Nuclear Physics, Grants No. DE-FG88ER41450 and No. DE-SC0012704 (D.E.K., S.S., Y.-C.L.), No. DE-FG02-87ER40371 (M.B.), No. DE-FG02-92ER40713 (S.A.V.), No. DE-FG0201ER41195 (H.-U.Y.), and within the framework of the Beam Energy Scan Theory (BEST) Topical Collaboration.

- 
- [1] D. E. Kharzeev, The chiral magnetic effect and anomaly-induced transport, *Prog. Part. Nucl. Phys.* **75**, 133 (2014).
- [2] D. E. Kharzeev, K. Landsteiner, A. Schmitt, and H.-U. Yee, Strongly interacting matter in magnetic fields: An overview, *Lect. Notes Phys.* **871**, 1 (2013).
- [3] D. E. Kharzeev, J. Liao, S. A. Voloshin, and G. Wang, Chiral magnetic and vortical effects in high-energy nuclear collisions—A status report, *Prog. Part. Nucl. Phys.* **88**, 1 (2016).
- [4] V. A. Miransky and I. A. Shovkovy, Quantum field theory in a magnetic field: From quantum chromodynamics to graphene and Dirac semimetals, *Phys. Rep.* **576**, 1 (2015).
- [5] K. Landsteiner, Notes on anomaly induced transport, *Acta Phys. Pol. B* **47**, 2617 (2016).
- [6] D. E. Kharzeev and J. Liao, Chiral magnetic effect reveals the topology of gauge fields in heavy-ion collisions, *Nat. Rev. Phys.* **3**, 55 (2021).
- [7] D. Kharzeev, Parity violation in hot QCD: Why it can happen, and how to look for it, *Phys. Lett. B* **633**, 260 (2006).
- [8] D. E. Kharzeev, L. D. McLerran, and H. J. Warringa, The effects of topological charge change in heavy ion collisions: ‘Event by event P and CP violation’, *Nucl. Phys. A* **803**, 227 (2008).
- [9] K. Fukushima, D. E. Kharzeev, and H. J. Warringa, The chiral magnetic effect, *Phys. Rev. D* **78**, 074033 (2008).
- [10] D. Kharzeev and A. Zhitnitsky, Charge separation induced by P-odd bubbles in QCD matter, *Nucl. Phys. A* **797**, 67 (2007).
- [11] J. Erdmenger, M. Haack, M. Kaminski, and A. Yarom, Fluid dynamics of R-charged black holes, *J. High Energy Phys.* **01** (2009) 055.
- [12] A. Vilenkin, Equilibrium parity violating current in a magnetic field, *Phys. Rev. D* **22**, 3080 (1980).
- [13] M. A. Metlitski and A. R. Zhitnitsky, Anomalous axion interactions and topological currents in dense matter, *Phys. Rev. D* **72**, 045011 (2005).
- [14] G. M. Newman and D. T. Son, Response of strongly-interacting matter to magnetic field: Some exact results, *Phys. Rev. D* **73**, 045006 (2006).
- [15] D. E. Kharzeev and H.-U. Yee, Chiral magnetic wave, *Phys. Rev. D* **83**, 085007 (2011).
- [16] A. Aristova, D. Frenklakh, A. Gorsky, and D. Kharzeev, Vortical susceptibility of finite-density QCD matter, *J. High Energy Phys.* **10** (2016) 029.
- [17] O. V. Teryaev and V. I. Zakharov, From the chiral vortical effect to polarization of baryons: A model, *Phys. Rev. D* **96**, 096023 (2017).
- [18] V. E. Ambrus and M. N. Chernodub, Hyperon–anti-hyperon polarization asymmetry in relativistic heavy-ion collisions as an interplay between chiral and helical vortical effects, *Eur. Phys. J. C* **82**, 61 (2022).
- [19] L. Adamczyk *et al.* (STAR Collaboration), Global  $\Lambda$  hyperon polarization in nuclear collisions: Evidence for the most vortical fluid, *Nature (London)* **548**, 62 (2017).
- [20] J. Adam *et al.* (STAR Collaboration), Polarization of  $\Lambda$  ( $\bar{\Lambda}$ ) Hyperons Along the Beam Direction in Au+Au Collisions at  $\sqrt{s_{NN}} = 200$  GeV, *Phys. Rev. Lett.* **123**, 132301 (2019).
- [21] T. Niida (STAR Collaboration), Global and local polarization of  $\Lambda$  hyperons in Au+Au collisions at 200 GeV from STAR, *Nucl. Phys. A* **982**, 511 (2019).
- [22] B. Fu, S. Y. F. Liu, L. Pang, H. Song, and Y. Yin, Shear-Induced Spin Polarization in Heavy-Ion Collisions, *Phys. Rev. Lett.* **127**, 142301 (2021).
- [23] F. Becattini, M. Buzzegoli, A. Palermo, G. Inghirami, and I. Karpenko, Local Polarization and Isothermal Local Equilibrium in Relativistic Heavy Ion Collisions, *Phys. Rev. Lett.* **127**, 272302 (2021).
- [24] D. E. Kharzeev and H.-U. Yee, Anomalies and time reversal invariance in relativistic hydrodynamics: The second order and higher dimensional formulations, *Phys. Rev. D* **84**, 045025 (2011).
- [25] M. Ammon, S. Grieninger, J. Hernandez, M. Kaminski, R. Koirala, J. Leiber, and J. Wu, Chiral hydrodynamics in strong external magnetic fields, *J. High Energy Phys.* **04** (2021) 078.
- [26] D. T. Son and P. Surowka, Hydrodynamics with Triangle Anomalies, *Phys. Rev. Lett.* **103**, 191601 (2009).
- [27] A. A. Anselm and A. A. Johansen, Radiative corrections to the axial anomaly, *Zh. Eksp. Teor. Fiz.* **49**, 185 (1989) [*JETP Lett.* **49**, 214 (1989)].
- [28] S. L. Adler, Anomalies to all orders, in *50 Years of Yang-Mills Theory*, edited by G. ’t Hooft (World Scientific, Singapore, 2005), pp. 187–228.
- [29] G. Kawahara, S. Kida, M. Tanaka, and S. Yanase, Wrap, tilt and stretch of vorticity lines around a strong thin straight vortex tube in a simple shear flow, *J. Fluid Mech.* **353**, 115 (1997).
- [30] J. M. Dahl, Tilting of horizontal shear vorticity and the development of updraft rotation in supercell thunderstorms, *J. Atm. Sci.* **74**, 2997 (2017).
- [31] D. T. Son and N. Yamamoto, Berry Curvature, Triangle Anomalies, and the Chiral Magnetic Effect in Fermi Liquids, *Phys. Rev. Lett.* **109**, 181602 (2012).
- [32] M. A. Stephanov and Y. Yin, Chiral Kinetic Theory, *Phys. Rev. Lett.* **109**, 162001 (2012).
- [33] J.-W. Chen, S. Pu, Q. Wang, and X.-N. Wang, Berry Curvature and Four-Dimensional Monopoles in the Relativistic Chiral Kinetic Equation, *Phys. Rev. Lett.* **110**, 262301 (2013).
- [34] S.-Z. Yang, J.-H. Gao, Z.-T. Liang, and Q. Wang, Second-order charge currents and stress tensor in a chiral system, *Phys. Rev. D* **102**, 116024 (2020).

- [35] T. Hayata, Y. Hidaka, and K. Mameda, Second order chiral kinetic theory under gravity and antiparallel charge-energy flow, *JHEP* **05** (2021) 023.
- [36] Y.-C. Liu, K. Mameda, and X.-G. Huang, Covariant spin kinetic theory I: Collisionless limit, *Chin. Phys. C* **44**, 094101 (2020); Erratum: **45**, 089001 (2021).
- [37] A. Palermo, M. Buzzegoli, and F. Becattini, Exact equilibrium distributions in statistical quantum field theory with rotation and acceleration: Dirac field, *J. High Energy Phys.* **10** (2021) 077.
- [38] G. S. Denicol, H. Niemi, E. Molnar, and D. H. Rischke, Derivation of transient relativistic fluid dynamics from the Boltzmann equation, *Phys. Rev. D* **85**, 114047 (2012); **91**, 039902(E) (2015).
- [39] See Supplemental Material at <http://link.aps.org/supplemental/10.1103/PhysRevC.106.L051902> for the detailed derivation of the siCME and siCVE coefficients in chiral kinetic theory and for their Kubo relations in the Zubarev approach.
- [40] Y. Hidaka and D.-L. Yang, Nonequilibrium chiral magnetic/vortical effects in viscous fluids, *Phys. Rev. D* **98**, 016012 (2018).
- [41] S. Shi, C. Gale, and S. Jeon, From chiral kinetic theory to relativistic viscous spin hydrodynamics, *Phys. Rev. C* **103**, 044906 (2021).
- [42] A. Hosoya, M.-A. Sakagami, and M. Takao, Nonequilibrium thermodynamics in field theory: Transport coefficients, *Ann. Phys. (NY)* **154**, 229 (1984).
- [43] F. Becattini, M. Buzzegoli, and E. Grossi, Reworking the Zubarev's approach to non-equilibrium quantum statistical mechanics, *Particles* **2**, 197 (2019).
- [44] D. N. Zubarev, A statistical operator for non stationary processes, *Sov. Phys. Doklady* **10**, 850 (1966).
- [45] D. N. Zubarev, A. V. Prozorkevich, and S. A. Smolyanskii, Derivation of nonlinear generalized equations of quantum relativistic hydrodynamics, *Theor. Math. Phys.* **40**, 821 (1979).
- [46] C. G. van Weert, Maximum entropy principle and relativistic hydrodynamics, *Ann. Phys. (NY)* **140**, 133 (1982).
- [47] D. N. Zubarev and M. V. Tokarchuk, Nonequilibrium thermo field dynamics and the method of the nonequilibrium statistical operator, *Teor. Mat. Fiz.* **88N2**, 286 (1991).
- [48] V. G. Morozov and G. Ropke, Zubarev's method of a nonequilibrium statistical operator and some challenges in the theory of irreversible processes, *Condens. Matter Phys.* **1**, 673 (1998).
- [49] F. Becattini, L. Bucciantini, E. Grossi, and L. Tinti, Local thermodynamical equilibrium and the beta frame for a quantum relativistic fluid, *Eur. Phys. J. C* **75**, 191 (2015).
- [50] X.-G. Huang, A. Sedrakian, and D. H. Rischke, Kubo formulae for relativistic fluids in strong magnetic fields, *Ann. Phys. (NY)* **326**, 3075 (2011).
- [51] F. Becattini and E. Grossi, Quantum corrections to the stress-energy tensor in thermodynamic equilibrium with acceleration, *Phys. Rev. D* **92**, 045037 (2015).
- [52] M. Buzzegoli, E. Grossi, and F. Becattini, General equilibrium second-order hydrodynamic coefficients for free quantum fields, *J. High Energy Phys.* **10** (2017) 091; Erratum: **07** (2018) 119.
- [53] M. Buzzegoli and F. Becattini, General thermodynamic equilibrium with axial chemical potential for the free Dirac field, *J. High Energy Phys.* **12** (2018) 002; Erratum: **03** (2022) 45.
- [54] A. Harutyunyan, A. Sedrakian, and D. H. Rischke, Relativistic dissipative fluid dynamics from the non-equilibrium statistical operator, *Particles* **1**, 155 (2018).
- [55] M. Buzzegoli, Thermodynamic equilibrium of massless fermions with vorticity, chirality and electromagnetic field, *Lect. Notes Phys.* **987**, 53 (2021).
- [56] A. Harutyunyan, A. Sedrakian, and D. H. Rischke, Relativistic second-order dissipative hydrodynamics from Zubarev's non-equilibrium statistical operator, *Ann. Phys. (NY)* **438**, 168755 (2022).
- [57] E. Grossi, Local thermodynamical equilibrium for a quantum relativistic fluid, Ph.D. thesis, Florence University, 2014 (unpublished).
- [58] T. S. Evans, Three point functions at finite temperature, *Phys. Lett. B* **249**, 286 (1990).
- [59] T. S. Evans, N point finite temperature expectation values at real times, *Nucl. Phys. B* **374**, 340 (1992).
- [60] S. A. Voloshin, Parity violation in hot QCD: How to detect it, *Phys. Rev. C* **70**, 057901 (2004).
- [61] D. E. Kharzeev and D. T. Son, Testing the Chiral Magnetic and Chiral Vortical Effects in Heavy Ion Collisions, *Phys. Rev. Lett.* **106**, 062301 (2011).
- [62] Y. Jiang, S. Shi, Y. Yin, and J. Liao, Quantifying the chiral magnetic effect from anomalous-viscous fluid dynamics, *Chin. Phys. C* **42**, 011001 (2018).
- [63] S. Shi, Y. Jiang, E. Lilleskov, and J. Liao, Anomalous chiral transport in heavy ion collisions from anomalous-viscous fluid dynamics, *Ann. Phys. (NY)* **394**, 50 (2018).
- [64] S. Shi, H. Zhang, D. Hou, and J. Liao, Signatures of Chiral Magnetic Effect in the Collisions of Isobars, *Phys. Rev. Lett.* **125**, 242301 (2020).
- [65] B. Schenke, S. Jeon, and C. Gale, Elliptic and Triangular Flow in Event-by-Event (3+1)D Viscous Hydrodynamics, *Phys. Rev. Lett.* **106**, 042301 (2011).
- [66] C. Gale, S. Jeon, and B. Schenke, Hydrodynamic modeling of heavy-ion collisions, *Int. J. Mod. Phys. A* **28**, 1340011 (2013).
- [67] S. Schlichting and S. Pratt, Charge conservation at energies available at the BNL Relativistic Heavy Ion Collider and contributions to local parity violation observables, *Phys. Rev. C* **83**, 014913 (2011).
- [68] J. Liao, V. Koch, and A. Bzdak, Charge separation effect in relativistic heavy ion collisions, *Phys. Rev. C* **82**, 054902 (2010).
- [69] S. K. Singh and J.-E. Alam, Suppression of thermal vorticity as an indicator of QCD critical point, [arXiv:2110.15604](https://arxiv.org/abs/2110.15604).
- [70] K. Ikeda, D. E. Kharzeev, and Y. Kikuchi, Real-time dynamics of Chern-Simons fluctuations near a critical point, *Phys. Rev. D* **103**, L071502 (2021).
- [71] M. A. Stephanov, K. Rajagopal, and E. V. Shuryak, Signatures of the Tricritical Point in QCD, *Phys. Rev. Lett.* **81**, 4816 (1998).
- [72] X. An *et al.*, The BEST framework for the search for the QCD critical point and the chiral magnetic effect, *Nucl. Phys. A* **1017**, 122343 (2022).